Structure and photophysics of near-infrared emissive ytterbium(III) monoporphyrinate acetate complexes having neutral bidentate ligands†

Hongshan He,*[a] Andrew G. Sykes,[b] P. Stanley May[b] and Guishan He[c]

Received 11th May 2009, Accepted 16th June 2009
First published as an Advance Article on the web 27th July 2009
DOI: 10.1039/b909243a

Substitution reactions between [Yb(TPP)($OOCCH_3$)(CH_3OH)$_2$] (**1**) and neutral bidentate ligands NN led to the formation of monoporphyrinate ytterbium(III) complexes [Yb(TPP)($OOCCH_3$)(NN)] (TPP = 5,10,15,20-tetraphenylporphyrinate anion; NN = 4-methyl-1,10-phenanthroline (**2**), 1,10-phenanthroline (**3**), 4,7-dimethyl-1,10-phenanthroline (**4**), 5,6-epoxy-5,6-dihydroxy-1,10-phenanthroline (**5**) and 2,2′-dipyridylamine (**6**)). Single-crystal X-ray diffraction analysis revealed that ytterbium(III) ions in **1** and **6** were seven-coordinate with $OOCCH_3^-$ in monodentate coordination, whereas those in **2**, **3**, **4** and **5** were eight-coordinate with $OOCCH_3^-$ in bidentate coordination. The visible emission (650 and 720 nm) from the porphyrin and near-infrared (NIR) emission (980 and 1003 nm) from ytterbium(III) ion were observed for all complexes. The eight-coordinate complexes exhibited stronger NIR emission and longer lifetimes in toluene solution than the seven-coordinate complexes. The NIR emission of complexes with decreased lifetimes was also observed when they were blended into organic polymer PMMA.

Introduction

Monoporphyrinate lanthanide complexes have one porphyrinate dianion binding directly to the central metal ion with other ancillary ligands occupying the remaining coordination sites.[1–26] They are stable in air, soluble in most organic solvents, and have strong absorption in the UV-visible region. Ytterbium(III), erbium(III) and neodymium(III) complexes also exhibit characteristic emission in the near-infrared (NIR) region upon "sensitization", which makes them promising in medical diagnostics and photonics.[27–30] In medical diagnostics, they could be used as stable luminescence labels for bioassays, where transparency of NIR light to biological fluids provides an opportunity for high sensitivity techniques in early detection of tumor markers.[31,32] In photonics, erbium(III) and neodymium(III) are commonly used in optical fiber amplifiers due to their intra-4f transitions at 1550 and 1340 nm, respectively, which are two standard telecommunication wavelengths. By blending or doping these ions in optical fibers, the input signals can be amplified through laser principles for long-distance signal transmission.[31]

Development of new lanthanide complexes that emit efficiently in the NIR region is critical for diagnostic and photonic applications. During last several decades, research on monoporphyrinate lanthanide complexes has focused mainly on the acetylacetonate adducts, which were synthesized from reactions between porphyrin free bases and lanthanide acetylacetonate hydrates in 1,2,4-trichlorobenzene (TCB) at 215 °C as shown in eqn (1):[1,3]

$$H_2Por + Ln(acac)_3 \rightarrow [Ln(Por)(\eta^2\text{-acac})(Solv)] + 2Hacac \quad (1)$$

where Ln is the trivalent lanthanide ion, Por is the porphyrinate dianion, acac is the acetylacetonate anion and Solv is the solvent. This method has been used widely in the past, and in the present, for the preparation of their analogues.[11,33–42] The major problem is that the acac anion is very difficult to replace with other ancillary ligands for further functionalization. In addition, the acac anion could be cleaved through thermal pyrolysis resulting in acetate or propionate-coordinate complexes.[43,44] One solvent molecule (water or methanol) also coordinates to lanthanide ion leading to weak NIR emission due to the O–H oscillation.[45] In 1999, Wong[46] developed another method as shown in eqn (2):

$$H_2Por + Ln[N(SiMe_3)_2]_3 \cdot x[LiCl(THF)_3] \rightarrow [Ln(Por)(H_2O)_3]Cl \quad (2)$$

The interaction of porphyrin free base with lanthanide amide, followed by hydrolysis in the air, led to the formation of aqua-coordinated monoporphyrinate complexes [Ln(Por)(H_2O)$_3$]Cl (Ln = Yb^{3+}, Er^{3+}). The three water molecules were labile and could be replaced by anionic tripodal ligands forming stable neutral pseudo-"sandwich" complexes with a porphyrin ring and a tripodal ligand on each side.[19] The aqua complexes can also interact with each other and form dimers under neutral, acidic or basic conditions.[17] In 2003, a similar method for the preparation of pseudo-"sandwich" complexes was also reported by Reynolds *et al.*[47] The same authors also fabricated NIR OLEDs using these complexes and demonstrated their potential in photonics applications.[22] However, they lack other active groups for further functionalization and their preparation required an oxygen-free environment, which limited its applications. In addition, there

[a]*Center for Advanced Photovoltaics, Department of Electrical Engineering, South Dakota State University, Brookings, SD 57007, USA. E-mail: hongshan.he@sdstate.edu; Fax: 01 6056884401; Tel: 01-6056886962*
[b]*Department of Chemistry, University of South Dakota, Vermillion, SD 560069, USA. E-mail: asykes@usd.edu, Stanley.May@usd.edu; Fax: 01 6056776397; Tel: 01-6056775487*
[c]*Clinical Laboratory, Tumor Hospital of Gansu Province, Lanzhou, 730050, P. R. China*

† Electronic supplementary information (ESI) available: Fig. 1S: The decay curves of complex **4** in CD_3OD and CH_3OH. The excitation wavelength was 510 nm and decay was monitored at 978 nm. CCDC reference numbers 731407 (**4**), 731408 (**5**) and 731409 (**6**). For ESI and crystallographic data in CIF or other electronic format see DOI: 10.1039/b909243a

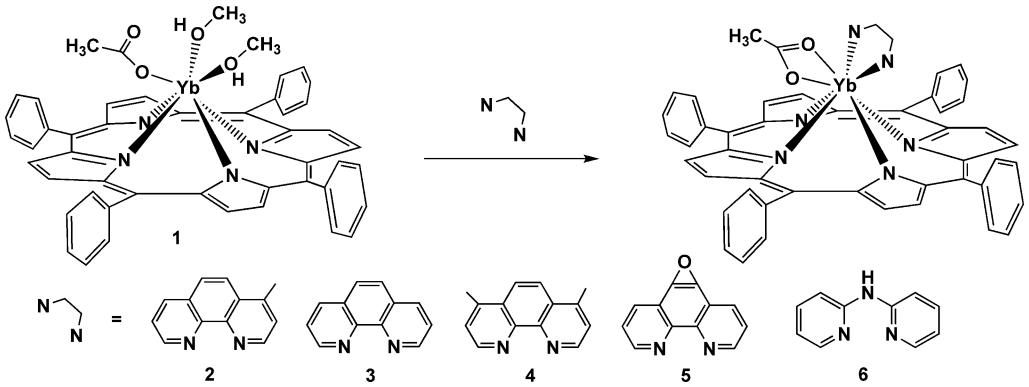

Scheme 1 Ytterbium(III) monoporphyrinate complexes.

are only a few tripodal ligands appropriate for the formation of pseudo-"sandwich" complexes

Recently we developed a method[48] to replace two water molecules in $[Yb(TPP)(H_2O)_3]Cl$ by protic bidentate ligands, but the remaining water still quenches the NIR emission. In 2001, García-Sánchez *et al.*[49] reported a monoporphyrinate lanthanide acetate from reaction (3):

$$H_2Por + Ln(OOCCH_3)_3 \cdot xH_2O \rightarrow [Ln(Por)(OOCCH_3)(Solv)_2] \quad (3)$$

It was proposed that the lanthanide ions were eight-coordinate with four nitrogen atoms from the porphyrinate dianion, two oxygen atoms from the chelating acetate anion, and two other atoms from solvent molecules. In a previous communication, we reported for the first time that the resulting complex $[Yb(TPP)(OOCCH_3)(CH_3OH)_2]$ was seven-coordinate with the $OOCCH_3^-$ anion in a monodentate coordination mode.[43] We also demonstrated the potential of this complex as a precursor for complexes with higher coordination numbers by its reaction with 4-methyl-1,10-phenanthroline.[43] In this report, we describe the details of this reaction, as shown in Scheme 1, structural analysis and photophysical properties of resulting complexes in solution and in an organic polymer matrix.

Experimental

Reagents and general procedures

5,10,15,20-Tetraphenylporphyrin (H_2TPP) was prepared according to the literature method.[50] Reagent grade ytterbium(III) acetate trihydrate, 1,10-phenanthroline (Phen), 4-methyl-1,10-phenanthroline (4-Me-Phen), 4,7-dimethyl-1,10-phenanthroline (4,7-Me-Phen) and 5,6-epoxy-5,6-dihydroxy-1,10-phenanthroline (EPO-Phen), 2,2′-dipyridylamine (DPA) and poly(methylmethaceylate) (PMMA) (MW = 123000) were obtained commercially and used without further purification. 1,2,4-Trichlorobenzene (TCB) was dried over molecular sieves overnight prior to use. All other chemicals and solvents for synthesis and purification were analytical grade and used as received. The solvents for photophysical studies were ACS grade, ultradry in Aeroseal containers and used as received. CD_3OD was from Cambridge Isotope Laboratories with 99.8% D in ampoule and used without further purification. $[Yb(TPP)(OOCCH_3)(CH_3OH)_2]$ (**1**) and $[Yb(TPP)(\eta^2\text{-}OOCCH_3)(\eta^2\text{-}4\text{-}Me\text{-}Phen)]$ (**2**) were prepared as we described previously.[43] Elemental compositions were determined on a Perkin Elmer Series II-2400 CHNS analyzer.

Preparation of $[Yb(TPP)(OOCCH_3)(NN)]$ (NN = Phen, 3; 4,7-Me-Phen, 4; EPO-Phen, 5; DPA, 6)

All complexes were prepared by a similar procedure. A typical procedure is given for $[Yb(TPP)(\eta^2\text{-}OOCCH_3)(Phen)]$ (**3**). To a toluene solution (20 mL) of **1** (24.2 mg, 0.027 mmol) was added an excess of 1,10-phenanthroline (20.2 mg, 0.11 mmol). The solution was magnetically stirred at room temperature for 12 h, and solvent was removed under reduced pressure. The crude product was then dissolved in dichloromethane and loaded on a column (silica gel) for purification. The column was flushed with dichloromethane and the first major band collected. After filtration, the volume of the solvent was reduced to ~1 mL and methanol (5 mL) was added. The purple solid was collected by filtration and dried under vacuum for 24 h. Yield: 23.1 mg, 86%. Calc. (found) for $C_{58}H_{41}N_6O_3Yb$ (**3**·CH_3OH): C, 66.79 (66.72); H, 3.96 (3.85); N, 8.06 (8.11%).

$[Yb(TPP)(\eta^2\text{-}OOCCH_3)(4,7\text{-}Me\text{-}Phen)]$ (**4**): 4,7-dimethyl-1,10-phenanthroline (20.5 mg, 0.10 mmol) and **1** (18.0 mg, 0.02 mmol) were used. Yield: 16.7 mg, 80%. Calc. (found) for $C_{61}H_{47}N_6O_3Yb$ (**4**·CH_3OH): C, 67.52 (67.88); H, 4.37 (4.35); N, 7.74 (7.74%).

$[Yb(TPP)(\eta^2\text{-}OOCCH_3)(EPO\text{-}Phen)]$ (**5**): 5,6′-epoxy-5,6-dihydroxy-1,10-phenanthroline (24.5 mg, 0.12 mmol) and **1** (24.6 mg, 0.027 mmol) were used. Yield: 25.1 mg, 89%. Calc. (found) for $C_{59}H_{43}N_6O_5Yb$ (**5**·CH_3OH·$5H_2O$): C, 65.07 (64.99); H, 3.98 (4.09); N, 7.72 (7.62%).

$[Yb(TPP)(OOCCH_3)(DPA)]$ (**6**): 2,2′-dipyridylamine (38.6 mg, 0.22 mmol) and **1** (23.0 mg, 0.025 mmol) were used. Yield: 22.0 mg, 85%. Calc. (found) for $C_{57}H_{44}N_7O_3Yb$ (**6**·CH_3OH): C, 65.32 (65.67); H, 4.23 (4.14); N, 9.36 (9.34%).

X-Ray crystallography

Single crystals were obtained by slow evaporation of dichloromethane–methanol solutions of the complexes at room temperature. The crystals were mounted on glass fibers before data collection. Diffraction measurements were made on a Bruker APEC II CCD detector at 125(2) K. The frames were collected with a scan width 0.3° in ω and integrated with Bruker SAINT software package using a narrow-frame integration algorithm. The unit cell was determined and refined by least squares upon

Table 1 X-Ray crystallographic data for **4**, **5** and **6**

	4	**5**	**6**
Empirical formula	$C_{60}H_{43}N_6O_2Yb$	$C_{59}H_{41}N_6O_4Yb$	$C_{58}H_{48}N_7O_4Yb$
M_r	1053.04	1071.02	1080.07
T/K	125(2)	125(2)	125(2)
λ/Å	0.71073	0.71073	0.71073
Crystal system	Triclinic	Triclinic	Triclinic
Space group	$P\bar{1}$	$P\bar{1}$	$P\bar{1}$
a/Å	10.2453(6)	9.766(2)	10.0590(12)
b/Å	13.4713(7)	13.559(3)	13.2450(15)
c/Å	18.5620(10)	17.444(3)	19.689(3)
α/°	74.6050(10)	82.934(3)	102.797(2)
β/°	89.8300(10)	89.885(3)	92.282(2)
γ/°	68.7340(10)	88.619(3)	111.7990(10)
V/Å^3	2289.3(2)	2291.7(8)	2353.5(5)
Z	2	2	2
D_c/g cm^{-3}	1.528	1.552	1.524
μ(Mo-Kα)/mm^{-1}	2.097	2.099	2.045
F(000)	1062	1078	1094
θ Range for data collection/°	1.69–25.39	1.80–25.70	1.71–25.52
Refl. collected/independent	23222/8417	8487/8487	23790/8637
R_{int}	0.0460	0.0000	0.0377
Data/restraints/parameters	8417/0/622	8487/0/631	8637/3/645
Goodness-of-fit on F^2	1.045	1.078	1.107
Final R indices [$I > 2\sigma(I)$]	$R1 = 0.0374$	$R1 = 0.0363$	$R1 = 0.0385$
	$wR2 = 0.0871$	$wR2 = 0.1029$	$wR2 = 0.1058$
R indices (all data)	$R1 = 0.0502$	$R1 = 0.0424$	$R1 = 0.0439$
	$wR2 = 0.0921$	$wR2 = 0.1061$	$wR2 = 0.1082$

the refinement of XYZ-centroids of reflections above $20\sigma(I)$. The data were corrected for absorption using the SADABS program.[51] The structures were refined on F^2 using the Bruker SHELXTL (version 5.1) software package.[52] A large residual density 0.55 Å from H60C of **4** was observed and was unable to be defined. The structural parameters are listed in Table 1.

Preparation of complex-blended polymer film

PMMA (0.5 g) was dissolved in chloroform (5 mL) and the solution was kept at room temperature overnight. Then to 0.5 mL of this solution was added 100 μL of **4** or **6** in toluene with concentration of 2.0×10^{-3} mol L^{-1}. The mixture was magnetically stirred for 2 h at room temperature, then dip-coated on microscopic glass slides (25 mm × 25 mm) with full coverage. The slides were placed on the bench, covered with plastic dishes, and left overnight. The films were then dried under vacuum for 24 h prior to measurements. The concentration of samples in the resulting PMMA films were 4×10^{-4} mmol per 100 mg of PMMA.

Photophysical measurements

Electronic absorption spectra in the UV-VIS region were recorded on a HP Agilent 5439 UV-Visible spectrophotometer using 1.0 cm quartz cell. Steady state luminescence spectra were obtained on a FS920 spectrometer (Edinburgh Instruments, Inc) with an arc lamp (Xe900) as light source. The Hamamatsu R928P and TE-cooled Hamamatsu G8605–23 detectors were used for UV-visible and NIR emission measurements, respectively. The instruments were PC-controlled through the F900 software, and the spectra were corrected from reference spectra of detectors. Decay curves of samples in the visible region were acquired on a LifeSpec II spectrometer (Edinburgh Instrument, Inc) using a time-correlated single photon counting technique. The intensities were monitored using a Hamamatsu H5773–02 detector. A pulse diode laser (EPL-375, Edinburgh Instruments, Inc) with excitation wavelength at 375 nm used as the light source and lifetimes were obtained by exponential fitting of deconvoluted data. The NIR decay curves were acquired using an optical parametric oscillator (OPOTEK Opolette) as an excitation source. NIR emission was detected using a 0.3 m flat-field monochromator (Jobin Yvon TRIAX 320) equipped with a NIR-sensitive photomultiplier tube (Hamamatsu R2658P) in a cooled housing (Products for Research). All spectra were corrected for instrumental function. The output from the photomultiplier was pre-amplified (Stanford Research SR 445A) and fed to a multichannel scaler (Stanford Research SR 430) for time-resolved photon counting. The entire system was PC controlled using LabView software.

Results and discussion

Preparation and structure of [Yb(TPP)(OOCCH$_3$)(NN)]

The precursor [Yb(TPP)(OOCCH$_3$)(CH$_3$OH)$_2$] (**1**) for the preparation of [Yb(TPP)(OOCCH$_3$)(NN)] was synthesized by direct reaction between ytterbium(III) acetate hydrate and H_2TPP in TCB at 210 °C for 48 h under N_2, followed by solvent exchange in methanol as we described previously.[43] In this precursor, the ytterbium(III) ion was seven-coordinate, with four nitrogen atoms from TPP^{2-}, two oxygen atoms from two CH$_3$OH molecules and one oxygen atom from the monodentate OOCCH$_3^-$ anion. The two methanol molecules were labile and were substituted by 1,10-phenanthroline derivatives and 2,2′-dipyridylamine, forming new ytterbium(III) complexes **2**–**6** with high yields. The resulting complexes were very stable in the air, had a bright purple color, and were soluble in dichloromethane, chloroform, toluene and slightly

soluble in methanol. Compositions of [Yb(TPP)(OOCCH$_3$)(NN)] complexes were confirmed by elemental analysis and single-crystal X-ray diffraction analysis.

The thermal ellipsoid diagrams of complexes **4**, **5** and **6** are shown in Fig. 1–3 and selected bond lengths and angles are listed in Table 2. In complexes **4** and **5**, Yb^{3+} is eight-coordinate, with four N atoms from the porphyrinate dianion, two N atoms from the 1,10-phenanthroline derivatives and two O atoms from acetate anion occupying the coordination sphere. The Yb^{3+} ions are located above the porphyrin ring with a distance to the mean N1/N2/N3/N4 plane of 1.1729(19) and 1.1691(19) Å for **4** and **5**, respectively. The phenanthroline ligands lie above two neighboring phenyl groups of TPP^{2-} with torsion angles between the two pyridyl groups of 14.75(0.34)° in **4** and 25.04 (0.19)° in **5**. The bite distances (N5···N6) are 2.662 and 2.652 Å for **4** and **5**, respectively. Complex **6** is seven-coordinate with acetate acting as a monodentate ligand and the Yb^{3+} ion is 1.1217 Å above the porphyrin ring. The torsion angle between the two pyridyl groups in DPA is 50.65(22)°, which is much higher than those observed in **2**, **4** and **5**. The bite distance (N5···N6) in **6** is 2.825 Å, which is 0.16 Å larger than those in **4** and **5**. This increase leads to a larger N5–Yb1–N6 angle and results in a monodentate coordination mode of the acetate anion in **6**. Hydrogen bonding interactions are observed in **5** and **6**. In **5**, one O atom of the acetate anion is hydrogen-bonded to one O atom of methanol solvent. In complex **6**, two methanol molecules are hydrogen-bonded to acetate oxygen (O2) and amino nitrogen (N7), respectively. They also form hydrogen bonds to each other by translation along the [1 1 0] direction forming one-dimensional chains as depicted in Fig. 3.

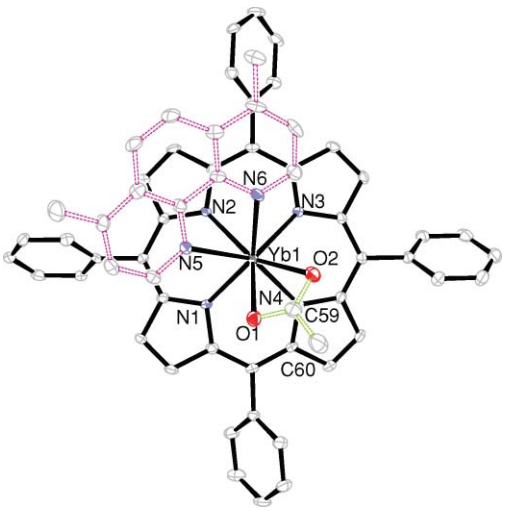

Fig. 1 The ORTEP diagram of [Yb(TPP)(η^2-OOCCH$_3$)(η^2-4,7-Me-Phen)] (**4**) with 50% thermal ellipsoid probability. The hydrogen atoms are omitted for clarity.

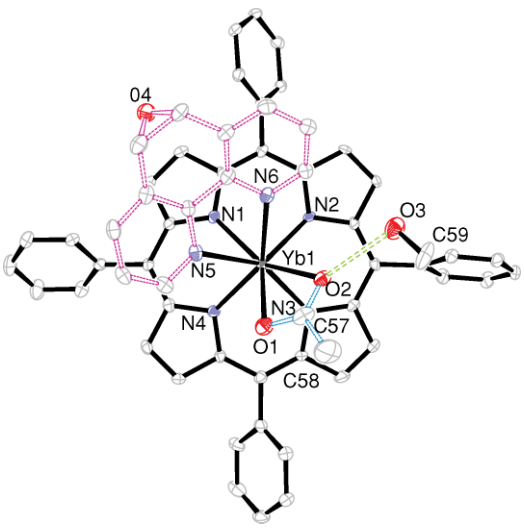

Fig. 2 The ORTEP diagram of [Yb(TPP)(η^2-OOCCH$_3$)(η^2-EPO-Phen)] (**5**) with 50% thermal ellipsoid probability. The hydrogen atoms are omitted for clarity; O2···O3 = 2.786 Å.

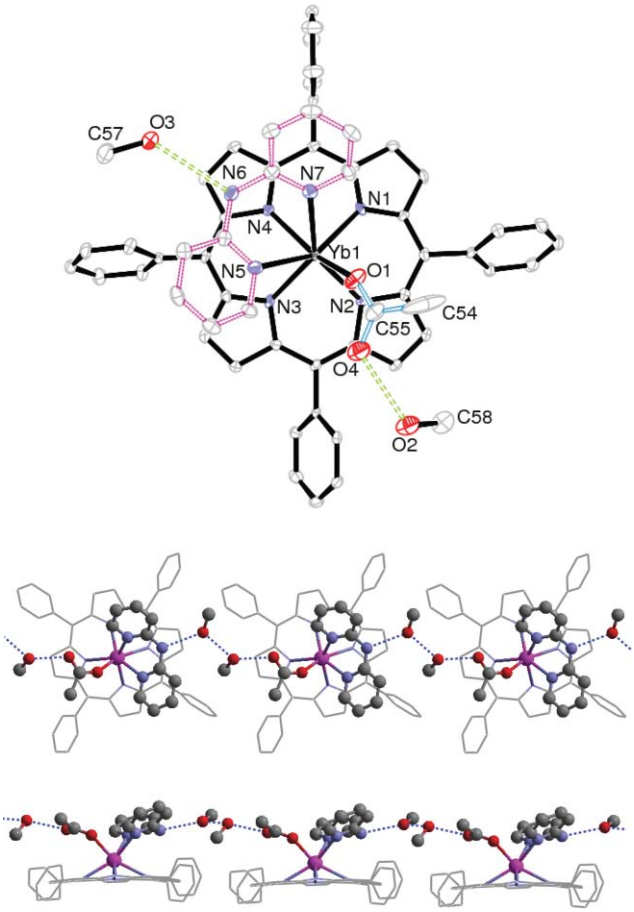

Fig. 3 Top: The ORTEP diagram of [Yb(TPP)(OOCCH$_3$)(η^2-DPA)]·2CH$_3$OH (**6**) with 50% thermal ellipsoid probability. The hydrogen atoms are omitted for clarity; O2···O4 = 2.711 Å, N7···O4 = 2.913 Å. Bottom: Packing diagram of hydrogen-bonding interaction between porphyrins viewed from top and side positions. Colour code: N, blue; O, red; Yb, purple; C, gray. The distance between O3 and O4 that are H-bonded in a chain structure is 2.738 Å.

The geometry of eight-coordinate complexes **2**, **3**, **4** and **5** can be described as square antiprismatic. Four N atoms (N1, N2, N3 and N4) from the porphyrin fall in one quadrilateral plane with the four inner angles close to 90°, whereas two acetate oxygen atoms (O1 and O2) and two phenanthroline nitrogen atoms (N5 and N6) lie in a trapezoidal plane due to the different bite distances in the acetate (O1···O2 ≈ 2.2 Å) and the phenanthroline (N5···N6 ≈ 2.7 Å). The two planes are nearly parallel to each

Table 2 Selected bond lengths and angles of **4**, **5** and **6**

4			
Yb1–N1	2.352(4)	N1–Yb1–N2	75.77(12)
Yb1–N2	2.376(4)	N2–Yb1–N3	75.03(13)
Yb1–N3	2.367(4)	N3–Yb1–N4	76.17(13)
Yb1–N4	2.355(4)	N1–Yb1–N4	75.95(13)
Yb1–N5	2.528(4)	N5–Yb1–N6	64.10(12)
Yb1–N6	2.488(4)	O1–Yb1–O2	54.68(11)
Yb1–O1	2.369(3)	O1–C59–O2	121.0(5)
Yb1–O2	2.418(3)		
5			
Yb1–N1	2.346(4)	N1–Yb1–N2	76.29(13)
Yb1–N2	2.338(4)	N2–Yb1–N3	75.72(13)
Yb1–N3	2.358(4)	N3–Yb1–N4	75.47(13)
Yb1–N4	2.359(4)	N1–Yb1–N4	75.21(13)
Yb1–N5	2.551(4)	N5–Yb1–N6	63.02(13)
Yb1–N6	2.523(4)	O1–Yb1–O2	54.45(12)
Yb1–O1	2.351(3)	O1–C57–O2	120.3(5)
Yb1–O2	2.437(3)		
6			
Yb1–N1	2.346(5)	N1–Yb1–N2	76.98(16)
Yb1–N2	2.351(4)	N2–Yb1–N3	76.63(15)
Yb1–N3	2.324(4)	N3–Yb1–N4	76.32(15)
Yb1–N4	2.342(4)	N1–Yb1–N4	76.96(16)
Yb1–N5	2.471(5)	N5–Yb1–N6	69.12(15)
Yb1–N6	2.508(5)	O1–C55–O2	123.7(6)
Yb1–O1	2.207(4)		

other with dihedral angles of 0.61(0.01), 0.90(0.20) and 0.28(0.19)° for **2**, **4** and **5**, respectively. The geometry of the seven-coordinate complex **6** is capped trigonal prismatic with O1 (acetate O) and N6 (phenanthroline N) in the cap positions, which are 1.8517(27) and 1.977(53) Å above the mean square planes of N1/N4/O5/O4 and N1/N4/N5/O1, respectively. The planarity of the porphyrin rings in these complexes is also quite different. The porphyrin rings of the synthesized complexes do not retain their planar geometry as observed in the H_2TPP free base and their Zn^{2+} and Cu^{2+} complexes. For eight-coordinate complexes, two torsion angles between the mean planes of the pyrrole rings on opposite sides of the porphyrin are different with one larger than another (29.04(26) *vs*. 2.97(48)° and 34.96(29) *vs*. 3.31(45)° for **4** and **5**, respectively), as a result, the porphyrin rings adopt an arched structure. In the seven-coordinate complexes, two pairs of pyrroles on opposite sides of the porphyrin bend almost equally away from the mean plane of N1N2N3N4 with torsion angles close to each other (14.90(46) *vs*. 11.48(44)° for **6**), resulting in a domed structure as observed in other seven-coordinate monoporphyrinate acetylacetonate lanthanide complexes and tripodal ligand-coordinated monoporphyrinate lanthanide complexes.[17–21]

Photophysical properties

The electronic absorption spectra of complexes **1–6** were characteristic of regular metalloporphyrins with a Soret band at about 430 nm and two Q bands centered at about 550 and 600 nm. This was in agreement with Gouterman's four-orbital model,[4] which predicts that four Q bands of the porphyrin free base will be reduced to two upon formation of a metalloporphyrin due to an increase in symmetry.[4] Upon excitation, all complexes give typical excitation and emission spectra in the visible region with a quantum efficiency (Φ) less than 0.005, which was significantly lower than that of H_2TPP (0.11) indicating the efficient intersystem crossing to its triplet state. All complexes also exhibited characteristic Yb^{3+} emission in the near-infrared region upon excitation, as shown in Fig. 4. In seven-coordinate complexes (**1** and **6**), a peak centered at approximately 975 nm with three weak shoulders at 950, 1000 and 1025 nm were observed. This feature is consistent with other seven-coordinate Yb^{3+} complexes we have described previously.[17–21,43,45,48,53] In eight-coordinate complexes (**2–5**) two strong peaks at 975 and 1005 nm, and a shoulder at 946 nm were observed. The substituents on 1,10-phenanthroline did not have a significant effect on emission efficiency, as shown in Fig. 5. It seemed that introducing an electron withdrawing group, such as an epoxy group in **5**, was unfavorable for NIR emission. The photophysical data are listed in Table 3.

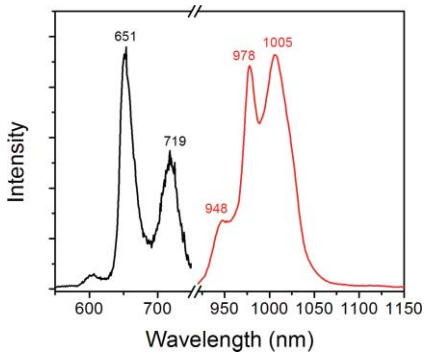

Fig. 4 Visible (black) and NIR (red) emission of **2** in toluene solution at room temperature (excitation wavelength = 375 nm; the intensity is normalized).

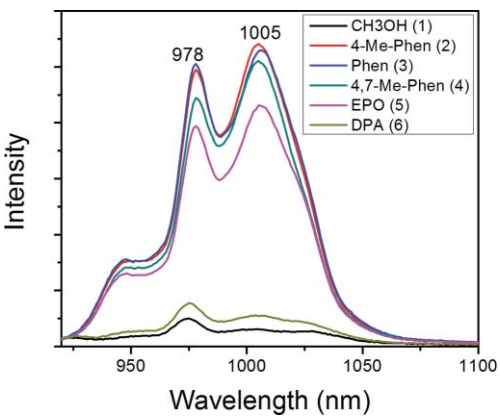

Fig. 5 Near-infrared emission spectra of complexes **1–6** in toluene at room temperature (excitation wavelength = 375 nm; concentration = 7.7×10^{-5} mol L^{-1}).

Several mechanisms have been proposed for sensitized NIR emission of ytterbium(III) complexes.[31] One that was proposed for monoporphyrinate lanthanide complexes was the Dexter mechanism.[31,54–57] In this mechanism porphyrin absorbs the light and is excited to its singlet state (S_1). The ligand then relaxes, *via* intersystem crossing, to a lower-lying triplet state (T_1), from which energy is transferred to the lanthanide ion *via* an exchange mechanism. The triplet state energy level of porphyrin is at ~15500 cm^{-1}, which is very favorable for energy transfer. To estimate the energy transfer rate, the emission of **4** in the presence of O_2 were recorded. Molecular oxygen is a quencher of the

Table 3 Photophysical data of monoporphyrinate ytterbium(III) complexes [YbTPP($OOCCH_3$)(NN)][a]

NN	Absorption, λ_{max}/nm (log ε)	Vis region		NIR region[e]	
		Emission, λ_{em}[b]/nm (τ[c]/ns)	Φ[d]	Emission, λ_{em}[b]/nm (τ[c]/ns)	Φ[f]
$2CH_3OH$ (**1**)	424 (5.53), 554 (4.18)	651 (6.70), 719	0.004	952, 975 (1.56), 1004, 1026,	1.30×10^{-3}
4-Me-Phen (**2**)	429 (5.38), 558 (4.12)	655 (8.20), 722	0.0008	949, 978 (17.29), 1005	14.4×10^{-3}
Phen (**3**)	429 (5.56), 557 (4.28)	653 (8.15), 722	0.0011	947, 978 (18.48), 1006	15.4×10^{-3}
4,7-Me-Phen (**4**)	430 (5.52), 558 (4.32)	651(10.14), 719	0.0052	948, 978 (17.82), 1005	14.85×10^{-3}
EPO-Phen (**5**)	427 (5.57), 557 (4.24)	651 (10.04), 719	0.0049	948, 978 (14.12), 1006	11.7×10^{-3}
DPA (**6**)	424 (5.68), 553 (3.68)	650 (9.14), 719	0.0018	950, 975 (11.60), 1006, 1023	9.66×10^{-3}
4 in PMMA	518, 558, 594	652, 722		951, 977 (12.6), 1003, 1015, 1024	10.5×10^{-3}
6 in PMMA	515, 555, 593	651, 721		950, 978 (10.8), 1003	8.75×10^{-3}

[a] All measurements were carried out in toluene at room temperature. [b] The excitation wavelength is 415 nm. [c] The excitation wavelength is 375 nm. [d] Tetraphenylporphyrin (H_2TPP) was used as reference standard ($\Phi = 0.11$ at 419 nm in toluene) and decay was monitored at 650 nm. [e] The decay was monitored at 978 nm. [f] Calculated according to $\Phi_{Yb} = \tau_{obs}/\tau_0$, where τ_0 is 1200 μs.

porphyrin triplet state resulting in the production of singlet oxygen that emits at ~1270 nm.[58] As shown in Fig. 6, no emission at ~1270 nm was observed for **4** after bubbling oxygen through an as-prepared toluene solution. In contrast a much stronger peak at 1270 nm was observed under similar condition for a solution of ZnTPP, which is known to have a high triplet yield and can transfer energy to molecular oxygen. This, together with very low emission efficiency of the complexes in the visible region, indicated that the energy transfer rate from the triplet state of the porphyrin to ytterbium(III) was faster than that to molecular oxygen. Due to the limitation of our instrument, it is difficult to obtain an accurate energy transfer rate; however, the rate is larger than the energy transfer rate to oxygen, *i.e.* 10^7 s^{-1}. This estimation is also consistent with other ytterbium(III) monoporphyrinate complexes.[31]

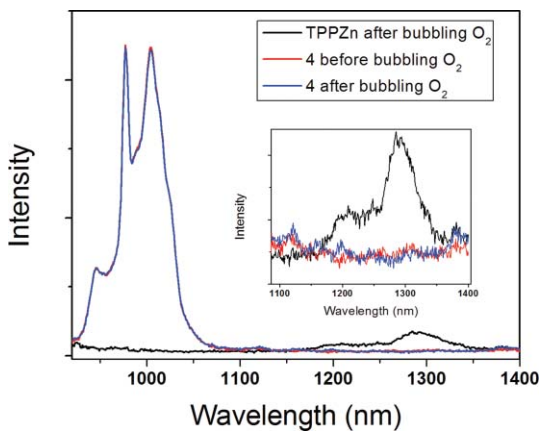

Fig. 6 Comparison of production of singlet oxygen from a toluene solution of **4** and ZnTPP upon excitation at 375 nm. The inset is the emission from singlet oxygen.

The overall NIR emission efficiency in solution was low. As indicated in Table 3, estimated quantum yields in toluene were less than 1% indicating the importance of the coordination environment on emission efficiency. The low emission efficiency is largely a result of the solvent interaction in the inner coordination sphere of ytterbium(III) ion. At the same concentration, the emission intensity of seven-coordinate complexes was six times less than that in eight-coordinate complexes as shown in Fig. 5. The emission lifetimes of complexes **2–5** are between 14 and 20 μs, which were much longer than those of **1** and **6**. For eight-coordinate complexes, no solvent molecule coordinates directly to metal center, whereas in seven-coordinate ones, solvents are present in the inner coordination sphere. In complex **1**, two methanols bind directly to the ytterbium(III) ion, resulting in dramatic quenching of NIR emission through increased multiphonon relaxation of the excited state of ytterbium(III). In complex **6**, no methanol coordinates directly to metal center; however, two methanol molecules are H-bonded to DPA and $OOCCH_3^-$; they are close to metal center, but further away compared to methanol molecules in complex **1**, therefore the quenching effect is reduced. Consistent with this observation was that the emission intensity of **5** with one methanol H-bonded to $OOCCH_3^-$ was weaker than that of **2** and **3** with no H-bonded methanol. It is also possible that **6** has a more open structure for the access of solvent to the inner coordination sphere. The results showed that methanol molecules in inner coordination sphere quench the NIR emission significantly. This can be attributed to the vibrational overtones of O–H in methanol with the NIR frequency.[15,59,60]

The outer-sphere interaction also played an important role in NIR emission. Fig. 7 showed the NIR emission of **4** in different solvents. The emission intensity in CH_3OH was four times weaker than that in toluene, indicating the interaction of methanol with Yb^{3+} in the complex. To identify whether this decrease comes from

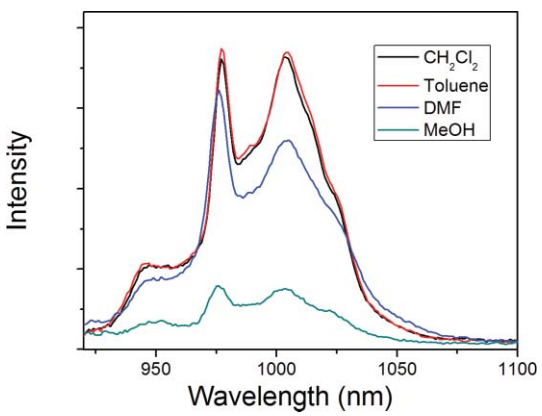

Fig. 7 Near-infrared emission spectra of **4** in different solvents at room temperature (excitation wavelength = 375 nm; concentration = 4.0×10^{-5} mol L^{-1}).

direct coordination of methanol to ytterbium(III), the lifetimes of single crystals of **4** that has no solvated methanol in the solid were measured in anhydrous CH_3OH and CD_3OD. The number of inner-sphere methanol molecules (q) was estimated from eqn (4) (developed by Beeby *et al.*[54]):

$$q_{Yb} = 2(\kappa_{CH_3OH} - \kappa_{CD_3OD} - B) \quad (4)$$

where B is a corrective factor, and κ is the decay rate in μs^{-1}. From the decay curves, as shown in Fig. S1 in the ESI,† the lifetimes at 978 nm in CH_3OH and CD_3OD were 7.2 and 17.2 μs, respectively. The calculated q values were close to zero, if B is between 0.05 and 0.1. This indicates that oscillators in the outer coordination sphere also quench the NIR emission in eight-coordinate complexes.[61] To further confirm this outer-sphere quenching effect, complexes **4** and **6** were blended into poly(methylmethaceylate) (PMMA), which is known to have a high percentage of C–H bonds.[22,33,62–66] The spectra were very similar to those in solution, as shown in Fig. 8. The lifetimes, as shown in the inset of Fig. 8, were 12.6 and 10.2 μs for **4** and **6** in PMMA, respectively. These values were lower than those obtained in toluene, but higher than that in methanol. The decrease relative to toluene may come from a clustering effect or from C–H oscillation of the PMMA. The clustering effect is common in lanthanide salt-doped polymers. Zheng *et al.*[67] studied the fluorescence of [Eu(DBM)(Phen)] (DBM = dibenzoylmethide) in PMMA and no clustering effect was observed. In our system, the ytterbium(III) was also encapsulated by a macrocyclic porphyrin ring and the resulting films exhibited high homogeneity; therefore it is unlikely that a clustering effect plays a significant role in quenching the NIR emission in PMMA. On the contrary, the decay curves fitted well with a single exponential function indicating the quenching effect mostly came from outer-sphere interaction. In this regard, the blending of these complexes into deuteriated or fluorinated polymers will be very beneficial for achieving high emission efficiency. Research in this area is ongoing.

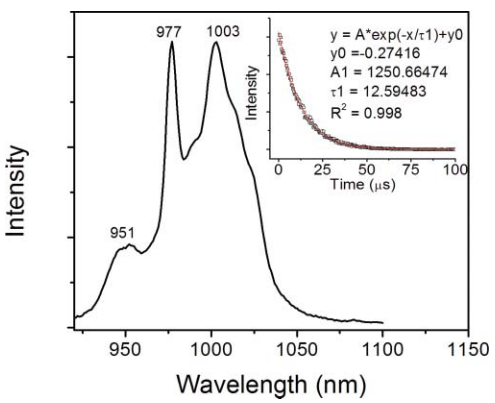

Fig. 8 Near-infrared emission spectra of PMMA film with 4×10^{-4} mol of **4** per 100 mg of PMMA. The inset is the luminescence decay of the film at 975 nm and the single exponential fitting (excitation wavelength = 510 nm).

Conclusion

Lanthanide porphyrinate complexes have broad applications in photovoltaics, diagnostics and photonics due to their strong absorption in the UV-visible region and their unique emission in the near-infrared region. In this report, we described structural and photophysical properties of several seven- and eight-coordinate ytterbium(III) tetraphenylporphyrinate complexes having diimines as ancillary ligands. The eight-coordinate complexes exhibited enhanced NIR emission and increased lifetime relative to the seven-coordinate species. The energy transfer from the triplet state of the porphyrin to the excited state of ytterbium(III) was faster than that to molecular oxygen. The NIR emission of seven-coordinate complexes is sensitive to solvent oscillators in both the inner- and outer-coordination spheres, whereas the emission of eight-coordinate complexes are only quenched by the less-effective outer-sphere solvent.

Acknowledgements

This material is based upon work supported by NSF/EPSCoR-0554609.

Notes and references

1 C.-P. Wong, R. F. Venteicher and W. D. Horrocks, Jr., *J. Am. Chem. Soc.*, 1974, **96**, 7149–7150.
2 W. D. Horrocks, Jr., R. F. Venteicher, C. A. Spilburg and B. L. Vallee, *Biochem. Biophys. Res. Commun.*, 1975, **64**, 317–322.
3 W. D. Horrocks, Jr. and C.-P. Wong, *J. Am. Chem. Soc.*, 1976, **98**, 7157–7162.
4 M. Gouterman, C. D. Schumaker, T. S. Srivastava and T. Yonetani, *Chem. Phys. Lett.*, 1976, **40**, 456–461.
5 W. D. Horrocks, Jr. and E. G. Hove, *J. Am. Chem. Soc.*, 1978, **100**, 4386–4392.
6 K. N. Solov'ev, G. F. Stel'makh, V. E. Pyatosin, K. N. Solovyov and T. F. Kachura, *Chem. Phys. Lett.*, 1980, **73**, 80–83.
7 K. Tatsumi and M. Tsutsui, *J. Am. Chem. Soc.*, 1980, **102**, 882–884.
8 C. P. Wong, *Inorg. Synth.*, 1983, **22**, 156–162.
9 A. G. Coutsolelos and G. A. Spyroulias, *Polyhedron*, 1994, **13**, 647–653.
10 G. Liu, T. Shi and X. Liu, *Polyhedron*, 1994, **13**, 2255–2258.
11 G. A. Spyroulias, M. P. Sioubara and A. G. Coutsolelos, *Polyhedron*, 1995, **14**, 3563–3571.
12 J. Jiang, L. Wei, P. Gao, Z. Gu, K.-I. Machida and G.-Y. Adachi, *J. Alloys Compd.*, 1995, **225**, 363–366.
13 W.-K. Wong, A. Hou, J. Guo, H. He, L. Zhang, W.-Y. Wong, K.-F. Li, K.-W. Cheah, F. Xue and T. C. W. Mak, *J. Chem. Soc., Dalton Trans.*, 2001, 3092–3098.
14 Z. X. Zhao, T. F. Xie, D. M. Li, D. J. Wang and G. F. Liu, *Synth. Met.*, 2001, **123**, 33–38.
15 Y. Korovin and N. Rusakova, *Rev. Inorg. Chem.*, 2001, **21**, 299–329.
16 M. Yu, L.-X. Yu, W.-P. Jian, W.-S. Yang and G.-F. Liu, *Chem. Res. Chin. Univ.*, 2004, **20**, 807–809.
17 H. He, X. Zhu, A. Hou, J. Guo, W.-K. Wong, W.-Y. Wong, K.-F. Li and K.-W. Cheah, *Dalton Trans.*, 2004, **23**, 4064–4073.
18 H. He, W.-K. Wong, K.-F. Li and K.-W. Cheah, *Synth. Met.*, 2004, **143**, 81–87.
19 H. He, J. Guo, Z. Zhao, W.-K. Wong, W.-Y. Wong, W.-K. Lo, K.-F. Li, L. Luo and K.-W. Cheah, *Eur. J. Inorg. Chem.*, 2004, 837–845.
20 H. He, W.-K. Wong, J. Guo, K.-F. Li, W.-Y. Wong, W.-K. Lo and K.-W. Cheah, *Inorg. Chim. Acta*, 2004, **357**, 4379–4388.
21 H. He, W.-K. Wong, J. Guo, K.-F. Li, W.-Y. Wong, W.-K. Lo and K.-W. Cheah, *Aust. J. Chem.*, 2004, **57**, 803–810.
22 B. S. Harrison, T. J. Foley, A. S. Knefely, J. K. Mwaura, G. B. Cunningham, T.-S. Kang, M. Bouguettaya, J. M. Boncella, J. R. Reynolds and K. S. Schanze, *Chem. Mater.*, 2004, **16**, 2938–2947.
23 M. Yu, G.-J. Chen and G.-F. Liu, *J. Phys. Chem. Solids*, 2007, **68**, 541–548.
24 W.-K. Wong, X. Zhu and W.-Y. Wong, *Coord. Chem. Rev.*, 2007, **251**, 2386–2399.
25 S. Fu, X. Zhu, G. Zhou, W.-Y. Wong, C. Ye, W.-K. Wong and Z. Li, *Eur. J. Inorg. Chem.*, 2007, 2004–2013.
26 F.-L. Jiang, W.-K. Wong, X.-J. Zhu, G.-J. Zhou, W.-Y. Wong, P.-L. Wu, H.-L. Tam, K.-W. Cheah, C. Ye and Y. Liu, *Eur. J. Inorg. Chem.*, 2007, 3365–3374.

27 P. R. Diamente and F. C. J. M. van Veggel, *J. Fluoresc.*, 2005, **15**, 543–551.
28 G. A. Hebbink, L. Grave, L. A. Woldering, D. N. Reinhoudt and F. C. J. M. van Veggel, *J. Phys. Chem. A*, 2003, **107**, 2483–2491.
29 L. H. Slooff, A. van Blaaderen, A. Polman, G. A. Hebbink, S. I. Klink, F. C. J. M. Van Veggel, D. N. Reinhoudt and J. W. Hofstraat, *J. Appl. Phys.*, 2002, **91**, 3955–3980.
30 S. I. Klink, L. Grave, D. N. Reinhoudt, F. C. J. M. van Veggel, M. H. V. Werts, F. A. J. Geurts and J. W. Hofstraat, *J. Phys. Chem. A*, 2000, **104**, 5457–5468.
31 S. Comby and J.-C. G. Bünzli, in *Handbook on the Physics and Chemistry of Rare Earths*, ed. J. Karl, A. Gschneidner, J.-C. G. Bünzli and V. K. Pecharsky, Elsevier, Amsterdam, 2007, vol. 37, pp. 217–470.
32 D. K. P. Ng, J. Jiang, K. Kasuga and K. Machida, in *Handbook on the Physics and Chemistry of Rare Earths*, eds. K. A. Gschneidner, Jr., L. Eyring and G. H. Lander, Elsevier, Amsterdam, 2007, vol. 32, pp. 611–653.
33 J. K. Mwaura, A. S. Knefely, K. S. Schanze, J. M. Boncella and J. R. Reynolds, *Polym. Prepr. (Am. Chem. Soc., Div. Polym. Chem.)*, 2004, **45**, 907–908.
34 G. K. Tsikalas and A. G. Coutsolelos, *Inorg. Chem.*, 2003, **42**, 6801–6804.
35 W. Huang, H. Xiang, Q. Gong, Y. Huang, C. Huang and J. Jiang, *Chem. Phys. Lett.*, 2003, **374**, 639–644.
36 H. Tsukube and S. Shinoda, *Chem. Rev.*, 2002, **102**, 2389–2403.
37 H. Tsukube, S. Shinoda and H. Tamiaki, *Coord. Chem. Rev.*, 2002, **226**, 227–234.
38 Z.-X. Zhao, Q.-H. Xu, D.-M. Li, G.-F. Liu, L.-S. Li and R.-R. Xu, *Solid State Sci.*, 2001, **3**, 339–345.
39 H. Sukube, M. Wada, S. Shinoda and H. Tamiaki, *J. Alloys Compd.*, 2001, **323–324**, 133–137.
40 G. A. Spyroulias, D. de Montauzon, A. Maisonat, R. Poilblanc and A. G. Coutsolelos, *Inorg. Chim. Acta*, 1998, **275–276**, 182–191.
41 L. L. Wittmer and D. Holten, *J. Phys. Chem.*, 1996, **100**, 860–868.
42 G. A. Spyroulias and A. G. Coutsolelos, *Polyhedron*, 1995, **14**, 2483–2490.
43 H. He and A. G. Sykes, *Inorg. Chem. Commun.*, 2008, **11**, 1304–1307.
44 G. A. Spyroulias, A. P. Despotopoulos, C. P. Raptopoulou, A. Terzis, D. de Montauzon, R. Poilblanc and A. G. Coutsolelos, *Inorg. Chem.*, 2002, **41**, 2648–2659.
45 H. He, A. G. Sykes, D. Galipeau, S. W. Ng and M. Ropp, *Inorg. Chem. Commun.*, 2008, **11**, 1051–1053.
46 W.-K. Wong, L. Zhang, F. Xue and T. C. W. Mak, *J. Chem. Soc., Dalton Trans.*, 1999, 3053–3062.
47 T. J. Foley, B. S. Harrison, A. S. Knefely, K. A. Abboud, J. R. Reynolds, K. S. Schanze and J. M. Boncella, *Inorg. Chem.*, 2003, **42**, 5023.
48 H. He, P. S. May and D. Galipeau, *Dalton Trans.*, 2009, 4766–4771.
49 M. A. García-Sánchez and A. Campero, *J. Non-Cryst. Solids*, 2001, **296**, 50–56.
50 A. D. Adler, F. R. Longo, J. D. Finarelli, J. Goldmacher, J. Assour and I. Korsakoff, *J. Org. Chem.*, 1967, **32**, 476.
51 G. M. Sheldrick, *SADABS, Empirical Absorption Correction Program*, University of Göttingen, Germany, 1997.
52 G. M. Sheldrick, *SHELXTLTM, Reference manual*, Version 5.1, Madison, WI, 1997.
53 H.-S. He, Z.-X. Zhao, W.-K. Wong, K.-F. Li, J.-X. Meng and K.-W. Cheah, *Dalton Trans.*, 2003, 980–986.
54 A. Beeby, I. M. Clarkson, R. S. Dickins, S. Faulkner, D. Parker, L. Royle, A. S. de Sousa, J. A. M. Williams and M. Woods, *J. Chem. Soc., Perkin Trans. 2*, 1999, 493–504.
55 A. Beeby, R. S. Dickins, S. FitzGenald, L. J. Govenlock, C. L. Maupin, D. Parker, J. P. Riehl, G. Siligardi and J. A. G. Williams, *Chem. Commun.*, 2000, 1183–1184.
56 S. Faulkner, A. Beeby, M. Carrie, A. Dadabhoy, A. M. Kenwright and P. G. Sammes, *Inorg. Chem. Commun.*, 2001, **4**, 187.
57 S. Faulkner, M.-C. Carrie, S. J. A. Pope, J. Squire, A. Beeby and P. G. Sammes, *Dalton Trans.*, 2004, 1405–1409.
58 H. Ke, W.-K. Wong, W.-Y. Wong, H.-L. Tam, C.-T. Poon and F. Jiang, *Eur. J. Inorg. Chem.*, 2009, 1243–1247.
59 T. Gunnlaugsson and F. Stomeo, *Org. Biomol. Chem.*, 2007, **5**, 1999–2009.
60 A. Dossing, *Eur. J. Inorg. Chem.*, 2005, 1425–1434.
61 P. Stanley May and F. S. Richardson, *Chem. Phys. Lett.*, 1991, **179**, 277–281.
62 Y. Hasegawa, K. Sogable, Y. Wada, T. Kitamura, N. Nakashima and S. Yanagida, *Chem. Lett.*, 1999, 35–37.
63 L. H. Slooff, A. Polman, S. I. Klink, G. A. Hebbink, L. Grave, F. C. J. M. van Veggel, D. N. Reinhoudt and J. W. Hofstraat, *Opt. Mater.*, 2000, **14**, 101–107.
64 K. Kuriki, Y. Koike and Y. Okamoto, *Chem. Rev.*, 2002, **102**, 2347–2356.
65 J. M. Boncella, T. J. Foley, B. S. Harrison, K. S. Schanze, J. R. Reynolds, M. Bouguettaya, J. Shim, P. H. Holloway and S. Ramakrishnan, *PMSE Prepr.*, 2002, **86**, 72.
66 T. S. Kang, B. S. Harrison, M. Bouguettaya, T. J. Foley, J. M. Boncella, K. S. Schanze and J. R. Reynolds, *Adv. Funct. Mater.*, 2003, **13**, 205–210.
67 Z. Zheng, H. Ming, X. Sun and J. Xie, *Chin. Opt. Lett.*, 2005, **3**, 605–607.